

Electron-nucleon cross section in $(e, e'p)$ reactions

S. Pollock*

Department of Physics, CB 390, University of Colorado, Boulder, Colorado 80309-0446

H. W. L. Naus

Institute for Theoretical Physics, University of Hannover, Germany

J. H. Koch

*National Institute for Nuclear Physics and High Energy Physics (NIKHEF), Amsterdam
and Institute for Theoretical Physics, University of Amsterdam, Amsterdam, The Netherlands*

(Received 21 December 1995)

We examine commonly used approaches to deal with the scattering of electrons from a bound nucleon. Several prescriptions are shown to be related by gauge transformations. Nevertheless, due to current nonconservation, they yield different results. These differences reflect the size of the uncertainty that persists in the interpretation of $(e, e'p)$ experiments. [S0556-2813(96)02005-0]

PACS number(s): 25.30.Fj, 13.40.Gp, 14.20.Dh

I. INTRODUCTION

In the interpretation of electron-nucleus scattering experiments one must make a choice of how to describe the interaction between an electron and a bound nucleon. Only the scattering of an electron on a free, on-shell nucleon is determined model independently. The kinematics of the scattering on a bound, off-shell nucleon is necessarily different and therefore there exists no well-defined unique procedure for the theoretical description of the nuclear scattering process.

In trying to describe the nuclear reaction by means of the free electromagnetic current of the nucleon, assumptions have to be made. They lead to a nonconserved nuclear current, an unphysical feature that is usually remedied in an *ad hoc* fashion. The most commonly used “conserved current” (cc) prescription for the $(e, e'p)$ reaction was introduced by de Forest [1]. This prescription also makes it possible to factorize the plane-wave impulse approximation (PWIA) cross section into a part containing the electron-nucleon cross section and a nuclear structure part. By comparing some variations within this class of recipes, it is often concluded that the uncertainty due to this procedure is small and that “off-shell” effects are negligible.

Clearly, this last point needs to be critically examined before one can draw conclusions from, e.g., $(e, e'p)$ experiments about subtle or exotic effects, either concerning nuclear structure or the influence of the medium on the reaction mechanism. An example of a reaction where this consideration enters is the recent $(e, e'p)$ measurement by Makins *et al.* [2]. It was motivated by the suggestion of a particular medium effect, color transparency.

It is the purpose of this work to briefly review the various approximations which go into the standard descriptions of the $(e, e'p)$ reaction and result in a nonconserved nuclear current. We discuss in detail prescriptions to restore conservation of the electromagnetic current of the off-shell nucleon

and relate them to particular choices of a gauge. Since there is much interest in the $(e, e'p)$ experiment by Makins *et al.* [2], we give examples for the kinematics of this experiment even though they are at the peak of the quasielastic cross section and the initial nucleon is not far off its mass shell. Our general conclusion is that the ambiguities connected to the electromagnetic current of an off-shell nucleon cannot be dismissed even if predictions among some currently used prescriptions are in close agreement.

II. CURRENT CONSERVING PRESCRIPTIONS

There has been considerable work on general aspects of the electromagnetic interaction with the nucleons in a nucleus (see, e.g., [3–8]). The nuclear wave function, the electromagnetic vertex and, e.g., the final state interaction need to be dealt with consistently. We will not repeat this discussion here and comment only on the assumptions that go into the often used recipe by de Forest [1] for the cross section for a bound, off-mass-shell nucleon. They are good examples for the problems one encounters in general and for the approximations one makes in practice.

The general form of the nuclear current is

$$J_{\mu} = \Psi_f^* \Gamma_{\mu} \Psi_i, \quad (1)$$

where $\Psi_{i,f}$ denote the initial and final wave functions and Γ_{μ} is the electromagnetic vertex operator. It is quite common to consider only the contributions due to one-body currents. In practice, to obtain a manageable description additional *ad hoc* assumptions are made concerning the wave functions, the vertex operator, the kinematics and current conservation. For simplicity, we will consider the $(e, e'p)$ reaction in PWIA, where the initial nucleon is bound and the final one is in a plane-wave, on-mass-shell state.

Wave function: The assumption made in Ref. [1] is that the wave function of both the plane-wave final nucleon and also the initial bound nucleon is given by the Dirac spinor for an on-shell nucleon. For the initial nucleon it is assumed that

*Electronic address: pollock@lucky.colorado.edu

this spinor is determined through its three-momentum, \vec{p} , the missing momentum of the initial nucleon, and the corresponding on-shell energy, $E_{\text{on}} = \sqrt{\vec{p}^2 + M^2}$.

Vertex operator: The general vertex for an off-shell nucleon, appearing between the nucleon wave functions, has been discussed in the literature, e.g., in Ref. [9]. The operator structure can be much more complex than the one one encounters in expressions for the free current. Furthermore, the associated form factors can depend in addition to q^2 , the photon four-momentum, on other scalar variables such as the invariant mass of the initial nucleon, p^2 . Rather than using this general expression (which would prevent factorization), all commonly used recipes make use of the free current. However, there are a variety of ways to write the free on-shell current in terms of two independent vertex operators and associated form factors. de Forest uses two forms:

$$J_1^\mu = e\bar{u}(\vec{p}') \left\{ [F_1(q^2) + F_2(q^2)] \gamma^\mu - F_2(q^2) \frac{(p+p')^\mu}{2M} \right\} u(\vec{p}), \quad (2)$$

and

$$J_2^\mu = e\bar{u}(\vec{p}') \left\{ F_1(q^2) \gamma^\mu + F_2(q^2) \frac{i\sigma^{\mu\nu} q_\nu}{2M} \right\} u(\vec{p}), \quad (3)$$

which can be transformed into each other by means of the Gordon decomposition. While for on-shell nucleons the two currents are equivalent, the results obtained when one tries to use them in the off-shell case are different.

Kinematics: In the $(e, e'p)$ reaction the energy transfer by the electron, ω , and the energy of the detected nucleon, E' , determine the energy of the initial bound nucleon to be $E = E' - \omega \neq E_{\text{on}}$. However, the use of a free on-shell spinor in the construction of the current involves the on-shell energy E_{on} for the initial nucleon. In the current based on Eq. (2), the energy of the initial nucleon also appears explicitly not only in the spinor, but also in the vertex operator and the usual prescription is to use E_{on} in the operator. An alternative is discussed in Ref. [4].

Current conservation: After the above manipulations, it is clear that the resulting current is not conserved. The last step then is to make the current conserved by hand. We will discuss three possibilities to do this and apply these methods to the two ways to write the free on-shell current, Eqs. (2) and (3).

(a) The method chosen in Ref. [1] is to replace the longitudinal component J_q , parallel to \vec{q} , by the charge density J_0 :

$$J_q \rightarrow J'_q = \frac{\omega J_0}{|\vec{q}|}, \quad (4)$$

and thus work with a four-current

$$J_\mu^{(\wedge)} = \left(\vec{J}_t, \frac{\omega J_0}{|\vec{q}|}, J_0 \right). \quad (5)$$

This would be correct and of no consequence if the current indeed was conserved. It has been argued that Siegerts theorem suggests this substitution when the current is not exactly conserved, but this long wavelength argument does not apply for the one-body current one is concerned with here, nor can it be expected to hold at the energies we consider below. The cross sections arising from this recipe, the often used prescriptions by de Forest, will be referred to simply as “ σ_{cc} ”.

(b) Of course, one could take care of current conservation in the opposite way by eliminating the charge density instead [4, 10]:

$$J_0 \rightarrow J'_0 = \frac{\vec{J} \cdot \vec{q}}{\omega}, \quad (6)$$

and to use

$$J_\mu^{(0)} = \left(\vec{J}, \frac{\vec{J} \cdot \vec{q}}{\omega} \right). \quad (7)$$

The resulting cross section will be referred to as σ_{cc}^0 .

(c) In other recipes [11] one subtracts a term proportional to q_μ to obtain a divergence free current:

$$J_\mu \rightarrow J_\mu^{(q)} = J_\mu - \frac{J \cdot q}{q^2} q_\mu. \quad (8)$$

The cross section obtained from this recipe will be referred to as σ_{cc}^q .

Connection to the gauge choice: As will be shown below, these different ways to restore current conservation can be seen as a choice of a gauge, which in principle should have no effect on the results. That these choices lead to different results shows the inconsistencies inherent in the commonly chosen approach to deal with the electromagnetic interaction of bound nucleons. The electron scattering matrix element can be written as

$$M = j^\mu \Pi_{\mu\nu} J^\nu, \quad (9)$$

where Π denotes the photon propagator and j the electron current. The explicit form of the propagator is gauge dependent and, as a consequence, so is the form of the matrix element.

In the covariant Lorentz class of gauges one has

$$M_L = \frac{i}{q^2} \left(-j \cdot J + (1 - \xi) \frac{(q \cdot J)(q \cdot j)}{q^2} \right), \quad (10)$$

where ξ is a free gauge parameter. It is common practice to work in the Feynman gauge, $\xi = 1$. In this case, one obtains

$$M_F = \frac{i}{q^2} (-j \cdot J). \quad (11)$$

This of course is always the case in the covariant Lorentz gauges since the electron current, j , is conserved and the second term in Eq. (10) vanishes. We will now show that the matrix elements resulting from the above three modified “conserved” currents, Eqs. (5), (7), and (8), when used in

the Feynman gauge yield the same matrix elements one obtains with the original, nonconserved current, but evaluated in different gauges.

Coulomb gauge: The well-known Coulomb gauge is an example of a noncovariant gauge. Using the Coulomb gauge propagator for $\Pi_{\mu\nu}$, the general matrix element, Eq. (9), reduces to

$$M_C = \frac{i}{\vec{q}^2} j_0 J_0 + \frac{i}{q^2} \left(\vec{j} \cdot \vec{J} - \frac{(\vec{q} \cdot \vec{J})(\vec{q} \cdot \vec{j})}{\vec{q}^2} \right). \quad (12)$$

This is precisely the same matrix element one would obtain in the Feynman gauge, upon using the replacement given in Eq. (4). The second part of Eq. (12) is the contribution of the transverse parts of the current, defined as

$$\vec{J}_i = \vec{J} - \frac{\vec{q} \cdot \vec{J}}{q^2} \vec{q}. \quad (13)$$

Depending on whether one uses the current J_1^μ given in Eq. (3) or J_2^μ Eq. (2), one obtains σ_{cc1} and σ_{cc2} from M_C . These are the widely used cross sections proposed by de Forest [1].

Weyl gauge: Another noncovariant gauge is the Weyl (or temporal) gauge. Using the photon propagator in this gauge, the charge densities do not explicitly contribute to the matrix element:

$$M_W = \frac{i}{q^2} \left(\vec{j} \cdot \vec{J} - \frac{(\vec{q} \cdot \vec{J})(\vec{q} \cdot \vec{j})}{\omega^2} \right). \quad (14)$$

Again, it is readily seen that this is the same expression one would have obtained in the Feynman gauge upon using the replacement given in Eq. (6), yielding σ_{cc1}^0 or σ_{cc2}^0 , depending on the form for the on-shell current one used to approximate the off-shell current.

Landau gauge: Finally, another example from the covariant Lorentz class is the Landau gauge, defined by the gauge parameter $\xi=0$. As one can see from Eq. (10), this yields σ_{cc1}^q and σ_{cc2}^q , the same result as in the Feynman gauge with the *ad hoc* subtraction defined in Eq. (8) that guarantees a conserved current. In fact, one would obtain this result if one did nothing and simply used the original nonconserved current in Eq. (11).

Of course, physical observables should not depend on the choice of the gauge. Indeed, for conserved currents all the matrix elements given above can easily be shown to be equivalent. However, for nonconserved currents, i.e., broken gauge invariance, choosing a different gauge gives a different result. This is the situation for the approximation for the bound nucleon current: the results are not the same. The choice of which component to eliminate in favor of another or to simply make the *ad hoc* subtraction, Eq. (8), can thus be related to the choice of a gauge. The connection between a choice of the gauge and noncontributing parts of the currents is formally always present. However, it is only exact for conserved currents.

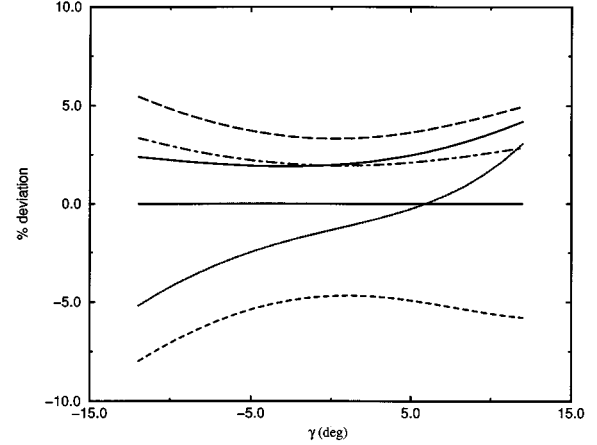


FIG. 1. Deviation of calculated cross sections from de Forest's "cc2" prescription as a function of the angle γ between the ejected proton and the momentum transfer direction. Here incident electron energy = 2.02 GeV, $Q^2=1.04$ GeV², $|\vec{q}|=1.2$ GeV, $|\vec{p}^-|=1.2$ GeV, and $E_m=47$ MeV at the center of the plot. Solid curve, σ_{cc1} ; dotted curve, σ_{cc1}^0 ; dashed curve, σ_{cc2}^0 ; long-dashed curve, σ_{cc1}^q ; dot-dashed curve, σ_{cc2}^q .

III. RESULTS AND CONCLUSIONS

Estimates of the differences between cc prescriptions: The formal connection between gauge choices and different cc prescriptions can be used for getting estimates of the uncertainties *within* the cc class. The starting point is that the nucleon current J is not conserved. Different matrix elements are obtained in noncovariant gauges. Since the electron current is conserved, all covariant Lorentz class gauges yield the same result. These differences between the cc recipes will be used below for different kinematics to get an impression of the uncertainty introduced by dealing with the off-shell current in an *ad hoc* fashion. It should be emphasized that the differences can only give a rough indication of these ambiguities as a function of the relevant kinematical variables. These estimates are not based on any dynamical input, but only on the connection between the cc prescriptions explained in the previous section.

A measure of how far one is from the on-shell kinematics is provided by the energy transfer. The actual energy transfer to the nucleon, ω , is determined by the electron kinematics. If the initial nucleon was on its mass shell, its energy E_{on} would be $(\vec{p}^2 + M^2)^{1/2}$, where \vec{p} is the missing momentum. The energy transfer, ω' , which one would have in that case is given by

$$\omega' = E' - E_{on}. \quad (15)$$

How far one is off shell is therefore indicated by the difference, $\Delta\omega$,

$$\Delta\omega = \omega - \omega'. \quad (16)$$

In Figs. 1–4 we show results for the off-shell electron-nucleon scattering cross section for the various cc choices. We choose kinematics which correspond roughly to the extremes of the kinematics sampled by Makins *et al.* [2]. Shown are the deviations of different prescriptions from

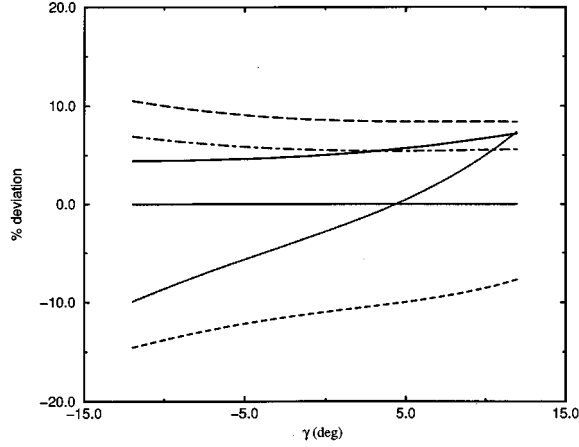


FIG. 2. Same as Fig. 1, but with outgoing proton momentum fixed at $|\vec{p}'|=1.08$ GeV, which reaches a larger missing energy (≈ 140 MeV at the center of the plot).

σ_{cc2} , the prescription used in Ref. [2] for the interpretation of their data. The cross sections are plotted as a function of γ , the angle [1] between the outgoing proton and the direction of \vec{q} . Positive γ corresponds to protons scattered *between* the incident beam direction and \vec{q} , negative γ is for protons scattered *beyond* \vec{q} . (The experimental data in Ref. [2] correspond to negative γ only.) All the figures assume that the recoil proton is in the electron scattering plane. Note that as $|\gamma|$ increases, the missing momentum generally also increases. We have chosen ranges of γ which correspond to missing momentum up to ≈ 250 MeV.

The electron scattering kinematics in Fig. 1 is $Q^2=1.04$ GeV², $|\vec{q}|=1.2$ GeV, and the cross sections are shown for $|\vec{p}'|=|\vec{q}|$, i.e., in perpendicular kinematics. The missing energy is 47 MeV at the center of the plot, and depends very weakly on γ . ($E_m=45$ MeV at $\gamma=\pm 12^\circ$.) The missing momentum ranges from 0 to 250 MeV/c, resulting in a $\Delta\omega$ from 47 to 80 MeV. The curves correspond to different prescriptions: how the current is made to be conserved (or which gauge is chosen) and which on-shell form for the cur-

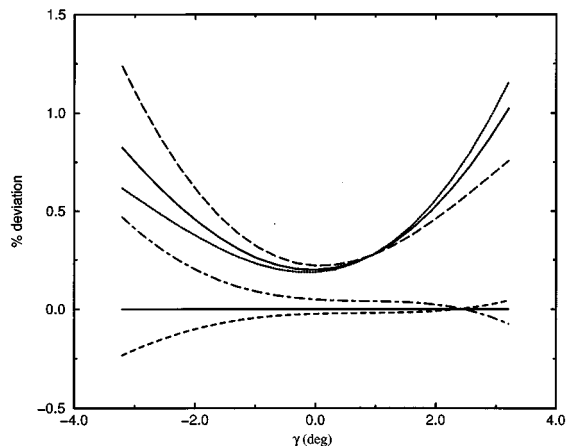


FIG. 3. Same as Fig. 1, but with incident energy = 5.12 GeV, $Q^2 = 6.77$ GeV², $|\vec{q}|=4.48$ GeV, $|\vec{p}'|=4.48$ GeV, and missing energy 9 MeV at $\gamma=0$ ($E_m = 6$ MeV at $\gamma=\pm 3^\circ$).

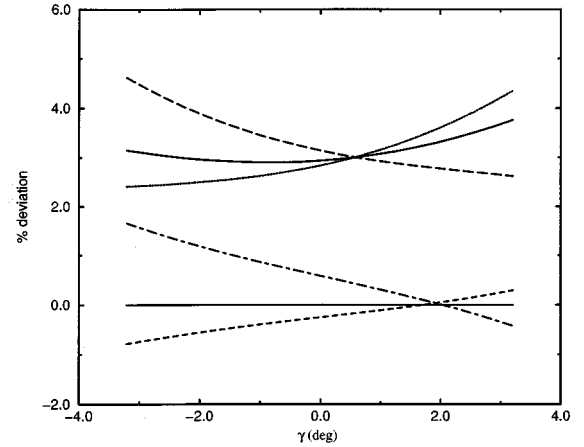


FIG. 4. Same as Fig. 3, but with outgoing proton momentum fixed at $|\vec{p}'|=4.35$ GeV, which reaches a large missing energy (≈ 137 MeV at the center of the plot).

rent is used to start with, Eq. (2) or (3). We see that there is a spread of more than $\pm 5\%$ among the different prescriptions relative to σ_{cc2} .

In Fig. 2, we fix the momentum of the knocked out nucleon at a value *lower* than $|\vec{q}|$, in order to access a larger missing energy. In this case, with $|\vec{p}'|$ reduced by 10% from its value in Fig. 1, the missing energy is approximately 140 MeV at $\gamma=0$, and the missing momentum ranges from 120 to 270 MeV/c. This leads to an increased $\Delta\omega$ between 148 and 180 MeV. Consequently, the largest difference between the cross sections grows to more than $\pm 10\%$.

In Fig. 3, we use the kinematics of the measurement with the highest incident energy: $Q^2=6.8$ GeV², $|\vec{q}|=4.5$ GeV, again in perpendicular kinematics with $|\vec{p}'|=|\vec{q}|$; the missing energy is 9 MeV at $\gamma=0$. In this case one is closer to the on-shell kinematics: $\Delta\omega$ is between 9 and 40 MeV and the differences between cross sections typically around 1%. In Fig. 4, $|\vec{p}'|$ is reduced (by 3%) to access a higher missing energy and momentum. In this case the missing energy is 137 MeV at $\gamma=0$, (135 MeV at $\gamma=\pm 3^\circ$) and the missing momentum ranges from 130 to 280 MeV/c, resulting in a $\Delta\omega$ from 148 to 179 MeV, comparable to Fig. 2, and the spread among the prescriptions grows to about 5%.

It should be stressed that variations of up to 10% occur solely due to the choice of gauge, indicating the severity of the approximations used to make the current conserved. The figures also illustrate another, somewhat smaller, uncertainty due to another assumption: differences between recipes labeled as 1 and 2, i.e., show the effect of choosing one of the two equivalent ways to write the on-shell current as given in Eqs. (2) and (3). For given electron kinematics, also this difference grows as we go away from on-shell kinematics, i.e., for larger $\Delta\omega$.

That the cross sections appear somewhat less sensitive to gauge choices at the higher energy kinematics can be understood from the following qualitative estimates which apply to a fixed choice of the on-shell current. A measure for the violation of current conservation is in each case given by [4]

$$q \cdot J = \omega J_0 - \vec{q} \cdot \vec{J} \equiv \chi, \quad \chi \approx \Delta\omega[J], \quad (17)$$

where the quantity $[J]$ denotes (part of) the nuclear current density. The matrix element in the Coulomb gauge, Eq. (12), is

$$M_C = \frac{-i}{q^2} j \cdot J + \frac{i}{q^2} \left(\frac{\omega j_0 \chi}{\vec{q}^2} \right). \quad (18)$$

Similarly, one obtains in the Weyl gauge, Eq. (14)

$$M_W = \frac{-i}{q^2} j \cdot J + \frac{i}{q^2} \left(\frac{j_0 \chi}{\omega} \right). \quad (19)$$

For conserved currents, such as with the subtraction in Eq. (8), we have $\chi=0$, and the matrix elements obviously reduce to the Feynman gauge matrix expression, Eq. (11). Since also the electron current is conserved, the matrix elements in all Lorentz gauges, such as Feynman and Landau gauge, are identical: $M_F = M_L$.

With the above expressions for the matrix elements, M_C , M_W , and M_L , we can estimate the relative differences between the various prescriptions. We start with comparing Coulomb and Lorentz gauges. Using Eqs. (11) and (18), one easily finds that

$$\frac{M_C - M_L}{M_L} \simeq - \frac{\omega j_0 \Delta \omega [J]}{\vec{q}^2 (j \cdot J)}. \quad (20)$$

For the purpose of getting order of magnitude estimates, we approximate $j_0 [J] \simeq j \cdot J$ and find

$$\frac{M_C - M_L}{M_L} \simeq - \frac{\omega \Delta \omega}{\vec{q}^2}. \quad (21)$$

For a given choice of the on-shell current this expression yields the right magnitude of the difference between the cross sections in the figures, i.e., the difference between $\sigma_{cc1,2}$ and $\sigma_{cc1,2}^q$. Similarly, one can obtain the corresponding expression for the Weyl gauge,

$$\frac{M_W - M_L}{M_L} \simeq - \frac{\Delta \omega}{\omega}, \quad (22)$$

which gives the right magnitude for the differences between $\sigma_{cc1,2}^0$ and $\sigma_{cc1,2}^q$. For the comparison of Coulomb and Weyl gauges, two noncovariant gauges, we can approximate the difference as

$$\frac{M_C - M_W}{M_C} \simeq \frac{-\omega \Delta \omega (1/\vec{q}^2 - 1/\omega^2)}{1 - \omega \Delta \omega / \vec{q}^2}. \quad (23)$$

In the kinematical region under consideration this can be further approximated by

$$\frac{M_C - M_W}{M_C} \simeq -\omega \Delta \omega \left(\frac{1}{\vec{q}^2} - \frac{1}{\omega^2} \right), \quad (24)$$

to obtain an estimate for the differences between $\sigma_{cc1,2}$ and $\sigma_{cc1,2}^0$. All the above estimates can explain the relative differences among the cross sections shown in the figures for the kinematics of the SLAC experiment; they also explain the larger differences found in other applications [4].

Our discussion does not provide any estimates for the differences between prescriptions based on different on-shell currents, only for different ways to restore current conservation. What we have shown are the effects due to different prescriptions in the literature for restoring current conservation that are used in the interpretation of $(e, e' p)$ experiments. We also showed the variation due to different on-shell equivalent electromagnetic currents. We have not discussed other aspects of scattering from a bound nucleon or showed the general framework in which all such aspects should be treated consistently, such as the nuclear wave function, final state interactions, or modifications of the electromagnetic vertex operator. The latter has been considered, e.g., in meson loop models and relatively small effects were found [12, 13]. Until a complete and fully consistent theoretical description of the $(e, e' p)$ reaction has been achieved, one really cannot know what a reasonable approximation would be and which of the prescriptions we discussed is ‘‘best.’’ The differences of the results we have shown give an idea of size of the present uncertainty in the interpretation of $(e, e' p)$ experiments.

ACKNOWLEDGMENTS

The work of J.H.K. was part of the research program of the Foundation for Fundamental Research of Matter (FOM) and the National Organization for Scientific Research (NWO). S.J.P. was supported by the U.S. DOE, and acknowledges the financial support of the Sloan Foundation.

-
- [1] T. de Forest, Jr., Nucl. Phys. **A392**, 232 (1983).
 [2] N.C.R. Makins *et al.*, Phys. Rev. Lett. **72**, 1986 (1994).
 [3] S. Frullani and J. Mougey, Adv. Nucl. Phys. **14**, 1 (1984).
 [4] H.W.L. Naus, S.J. Pollock, J.H. Koch, and U. Oelfke, Nucl. Phys. **A509**, 717 (1990).
 [5] H. Ito, W.W. Buck, and F. Gross, Phys. Rev. C **43**, 2483 (1991).
 [6] F. Gross and H. Henning, Nucl. Phys. **A537**, 344 (1992).
 [7] H. Henning, P.U. Sauer, and W. Theis, Nucl. Phys. **A537**, 367

- (1992).
 [8] X. Song, J.P. Chen, and J.S. McCarthy, Z. Phys. A **341**, 275 (1992).
 [9] A. M. Bincer, Phys. Rev. **118**, 855 (1960).
 [10] J.A. Caballero, T.W. Donnelly, and G.I. Poulis, Nucl. Phys. **A555**, 709 (1993).
 [11] J. Mougey *et al.*, Nucl. Phys. **A262**, 461 (1976).
 [12] H.W.L. Naus and J.H. Koch, Phys. Rev. C **36**, 2459 (1987).
 [13] P.C. Tiemeijer and J.A. Tjon, Phys. Rev. C **42**, 599 (1990).